

OPEN

Quadrupolar ordering and exotic magnetocaloric effect in RB_4 ($R = Dy, Ho$)

M. S. Song¹, K. K. Cho¹, B. Y. Kang¹, S. B. Lee² & B. K. Cho^{1*}

The interplay of charge, spin, orbital and lattice degrees of freedom has recently received great interest due to its potential to improve the magnetocaloric effect (MCE) for the purpose of magnetic cooling applications. Here, a new mechanism for a large entropy change with low magnetic fields in rare-earth tetraborides, especially for $Ho_{1-x}Dy_xB_4$ ($x = 0.0, 0.5, \text{ and } 1.0$), is proposed. For $x = 0.0, 0.5, \text{ and } 1.0$, the maximum entropy changes of the giant inverse MCE are found to be 22.7 J/kgK, 19.6 J/kgK, and 19.0 J/kgK with critical fields of 25 kOe, 40 kOe, and 50 kOe, respectively. For all compounds, systematic study on how the entropy changes as a function of the field and temperature is performed to investigate their correlation with consecutive double transitions, i.e., the magnetic dipolar order at $T = T_N$ and the quadrupolar order at $T = T_Q$ ($T_Q < T_N$). Based on Landau theory, it is found that this behaviour is attributed to the strong coupling between magnetic dipoles and quadrupoles in the presence of strong spin-orbit coupling and geometric frustration. Our work offers new insights into both academic and industrial interests in the discovery of giant MCE with various applications for magnetic cooling systems.

The magnetocaloric effect (MCE) is a thermodynamic property, in which heating or cooling occurs in magnetic materials when applying a magnetic field. For the conventional MCE, the cooling mechanism is based on the adiabatic demagnetization process. In contrast, the *inverse* situation can also occur, where the system is cooled via adiabatic magnetization. This is often termed as the *inverse* MCE. Refrigeration based on the conventional or inverse MCE is a solid-state cooling application, which is energy efficient, noise-free, and environmentally friendly. Thus, a large MCE is attractive as an alternative to conventional vapour refrigeration¹. In particular, a large MCE in a low-temperature region is being actively studied for the purpose of gas liquefaction (hydrogen and helium), space technology, and diverse scientific research technologies. In principle, the effective magnetic cooling using MCE can be achieved with the materials, which show large magnetic entropy change. Thus, for the development of novel solid-state cooling, the design and discovery of new materials that exhibit a large magnetic entropy change are important.

Intuitively, a large magnetic entropy is expected in materials with a first order magnetic phase transition accompanied with a spontaneous magnetization jump. However, this gives rise to heat loss during the refrigeration cycle due to the hysteresis, irreversibility and the narrow working temperature range. As another promising candidate, a system with geometrical frustration may contain an enormous ground state degeneracy due to competing spin exchange interactions, so a large magnetic entropy change is expected when a magnetic field is applied^{2–4}. In addition, more exotic scenarios with multipolar degrees of freedom and their influence on the entropy change have been proposed^{5–7}. Because such multipolar degrees of freedom are expected to give rise to an anomalous MCE, it would be of great interest to find such systems, thereby allowing us to unveil the nature of the anomalous MCE.

Multipolar degrees of freedom and their importance have garnered significant attention in many correlated electronic systems, such as heavy fermions, frustrated magnets, multiferroics and superconductivity^{8–13}. For alloys with heavy 4d, 5d transition metal ions or rare-earth ions, the spin and orbital degrees of freedoms are strongly entangled, and the system may contain a significant correlation between the spin-orbit coupled multipoles, resulting in their spontaneous ordering. When such multipolar degrees of freedom meet geometrical frustration, their interplay gives rise to multiple magnetic phase transitions, which significantly induces a large entropy change.

¹School of Materials Science and Engineering, Gwangju Institute of Science and Technology (GIST), Gwangju, 61005, Korea. ²Department of Physics, Korea Advanced Institute of Science and Technology (KAIST), Daejeon, 34141, Korea. *email: chobk@gist.ac.kr

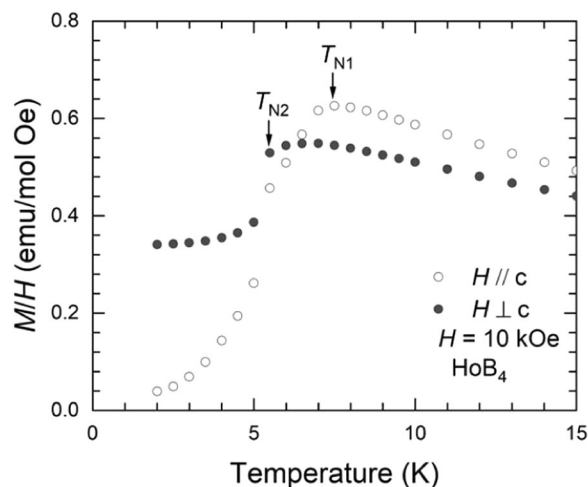


Figure 1. Temperature-dependent magnetization divided by an applied magnetic field, $H = 10$ kOe, parallel and perpendicular to the c -axis for HoB_4 .

even in the absence of a first order magnetic phase transition. Thus, exploring such multipolar degrees of freedom in a strongly spin-orbit coupled system is definitely required when investigating the potential candidate materials with a large MCE. Not only regarding technological applications, this also deepens our understanding of complicated spin systems in the presence of various competing exchange interactions and their exotic multipolar order, which is, in principle, very challenging to detect. Thus, it is often termed as the ‘hidden order’^{14–17}.

Motivated by the above, we propose a new candidate of material rare-earth tetraborides for a large *inverse* MCE, i.e., positive magnetic entropy change, and elucidate their theoretical origin, pursuing possible controllability. A rare-earth tetraboride with a chemical formula RB_4 ($R =$ rare-earth elements) is a system in which strong spin-orbit coupling and geometrical frustration coexist. In the presence of spin-orbit coupling and a crystalline electric field, the spin states in rare earth ions with valence $3+$ split into several doublets or singlets in terms of the total angular momentum J basis. It is known that, depending on rare-earth ions, four low lying energy states are quite well separated from the other excited states, forming pseudo-quartets^{18,19}. Furthermore, the lattice structure formed by R ions in the c plane is the Shastry-Sutherland lattice (SSL), which is a geometrically frustrated system, exhibiting double magnetic transitions, magnetic dipole ordering at $T = T_{N1}$ and quadrupolar ordering at $T = T_{N2}$ ²⁰. Since the 1970s, the physical properties and magnetic structure of RB_4 compounds have been studied^{21–25} and, recently, the detailed ground state of RB_4 ($R = \text{Dy}$, and Ho) was re-investigated by resonant X-ray scattering and X-ray and neutron diffraction^{18,26–29}. The two successive magnetic transitions of these compounds are related to the collinear antiferromagnetic transition at $T = T_{N1}$ along the c -axis, the quadrupolar ordering at $T = T_{N2}$ and the strong quadrupolar fluctuation between them. In addition, a structural transition from tetragonal to monoclinic is also observed at the quadrupolar ordering temperature, which indicates strong quadrupole-lattice coupling.

The field-induced entropy change of high-purity single crystals of RB_4 ($R = \text{Dy}$ and Ho) is investigated by examining the temperature- and field-dependence of magnetization with an applied field along the c -axis and the ab plane. It is quite remarkable that these materials exhibit a large entropy change in low fields, i.e., a maximum magnetic entropy change near the quadrupolar ordering of $+19.6$ J/kg·K, $+19.0$ J/kg·K, and $+22.7$ J/kg·K at the critical fields of 50 kOe, 40 kOe, and 25 kOe for DyB_4 , $\text{Dy}_{0.5}\text{Ho}_{0.5}\text{B}_4$, and HoB_4 , respectively. The exotic entropy change increases with an increasing magnetic field below the critical field but decreases above the critical field. The critical field is the regime where the non-collinear magnetic ground state breaks down, thus indicating that the entropy change is clearly correlated with the quadrupolar ordering.

Results and Discussion

Figure 1 shows the temperature-dependence of the magnetization divided by the applied magnetic field, parallel and perpendicular to the c -axis, namely, $M(T)/H$ with $H = 10$ kOe, for a single crystal of HoB_4 . There are two successive magnetic transitions at $T_{N2} = 5.7$ K and $T_{N1} = 7$ K for both applied magnetic fields parallel and perpendicular to the c -axis. Thus, this can be split into three distinct phases, I ($T > T_{N1}$), II ($T_{N1} > T > T_{N2}$), and III ($T_{N2} > T$) in the low-field region with a decreasing temperature. In phase I, the paramagnetic phase follows the Curies-Weiss law, $M(T)/H = C/(T - \theta)$, where $C = N_0 \mu_{\text{eff}}^2 / 3k_B$, N_0 is Avogadro’s number, k_B is the Boltzmann constant, and the effective magnetic moment, μ_{eff} , is determined to be $10.4 \mu_B$, where μ_B is the Bohr magneton, and the Weiss temperature, θ , is -12.7 K and -11.6 K for the magnetic field parallel and perpendicular to the c -axis, respectively. The μ_{eff} values are close to the theoretical value of Hund’s rule for the ground state of the isolated Ho^{3+} ions ($\mu_{\text{eff}} = 10.6 \mu_B$)^{28,30}. In phase II, it is known that the incommensurate magnetic order is dominant. However, the commensurate magnetic order evolves with a decreasing temperature, which also accompanies the elastic softening. In phase III, it is also reported that the quadrupolar ordering and magnetic dipole ordering coexist and the lattice distortion is also stabilized as a consequence of the strong quadrupole-strain interactions²⁸.

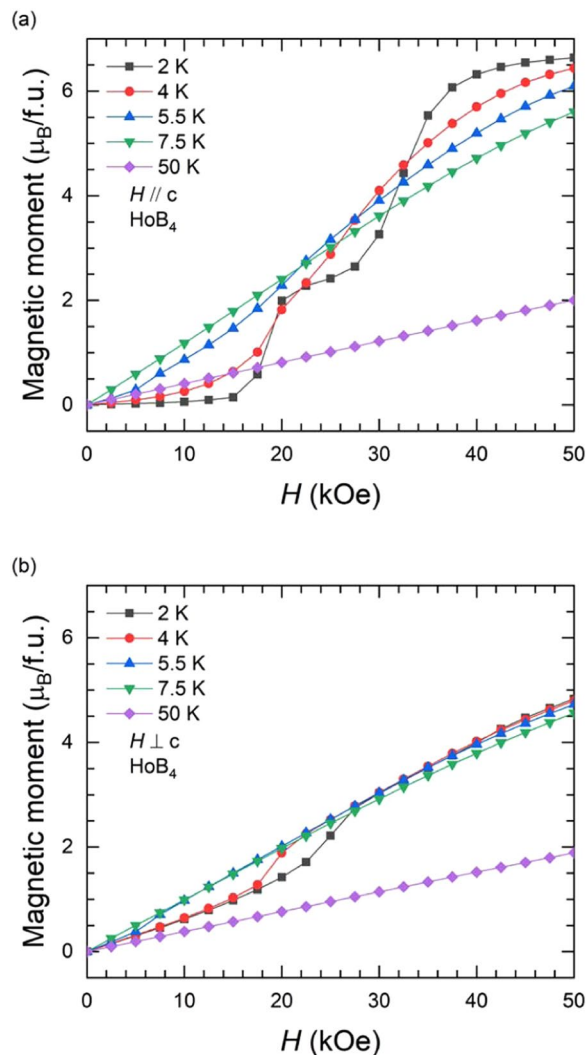


Figure 2. Magnetic field dependence of the isothermal magnetization at different temperatures in a range of $2\text{ K} \leq T \leq 50\text{ K}$ with applied field; (a) parallel and (b) perpendicular to the c -axis for HoB_4 .

Figure 2(a,b) show the isothermal magnetization curves at various temperatures in the range of $2\text{ K} \leq T \leq 50\text{ K}$ with a field applied along the c -axis and perpendicular to the c -axis for HoB_4 , respectively. The isothermal data, along the c -axis, at $T = 2\text{ K}$ show two meta-magnetic transitions at $H \approx 20\text{ kOe}$ and 35 kOe . The magnetic moment of the Ho^{3+} ion is $6.6\ \mu_B$ at $H = 50\text{ kOe}$, which is smaller than the maximum moment of the Ho^{3+} ion ($10.6\ \mu_B$). This indicates that the canted antiferromagnetic moments by the coupling between the quadrupolar moments and the magnetic dipole moments undergo a field-induced phase transition with an increasing field^{28,31}. Typical paramagnetic behaviour is observed at $T = 50\text{ K}$. On the other hand, the isothermal data, perpendicular to the c -axis, show similar but weaker meta-magnetic transition near $H \approx 20\text{ kOe}$ as compared to other configuration.

The magnetic entropy change, ΔS_M , can be estimated from the Maxwell equation in the approximated form

$$\Delta S_M(T, H) = \sum_i \frac{M_{i+1}(T_{i+1}, H) - M_i(T_i, H)}{T_{i+1} - T_i} \Delta H_i$$

where M_{i+1} and M_i are the experimentally measured values at temperatures T_{i+1} and T_i , respectively, in the magnetic field interval, $\Delta H_i = 0.25\text{ kOe}$. The temperature dependence of the magnetic entropy change of HoB_4 is calculated using isothermal magnetization data (Fig. 2) with a magnetic field applied along the c -axis and in the ab plane. These are plotted in Fig. 3(a,b), respectively. For the field applied along the c -axis, a large positive entropy change is observed below $T = T_{N1}$ with a maximum value of $22.7\text{ J/kg}\cdot\text{K}$ at $T = T_{N2}$ with the field change from 0 Oe to 25 kOe ($\Delta S_M(25\text{ kOe})$), as shown in Fig. 3(a). The maximum ΔS_M decreases with a further increase of the magnetic field. The entropy change at $T = T_{N2}$ with the field change from 0 Oe to 50 Oe ($\Delta S_M(50\text{ kOe})$), is relatively small compared to the value of $\Delta S_M(25\text{ kOe})$. The entropy change, $\Delta S_M(50\text{ kOe})$, near $T = T_{N1}$, which is negative, increases monotonically as the field increases, yielding $\Delta S_M = -15.9\text{ J/kg}\cdot\text{K}$ at $T = 8\text{ K}$, which is a typical characteristic of the conventional MCE. For the field applied along the ab plane, a positive entropy change,

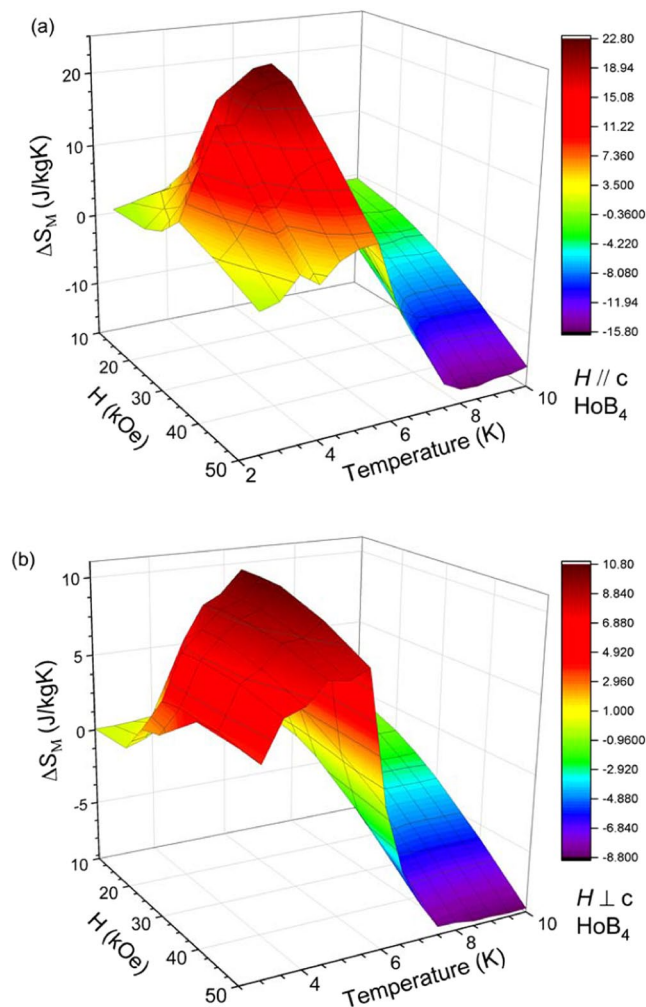


Figure 3. Temperature dependence of the magnetic entropy change in HoB₄ during various magnetic field changes of 10, 15, 20, 25, 30, 40 and 50 kOe; (a) parallel to the *c*-axis and (b) perpendicular to the *c*-axis.

ΔS_M (25 kOe), is observed with a maximum value of 10.75 J/kg·K near $T = T_{N2}$. At $T = T_{N1}$, the entropy change, ΔS_M (50 kOe), becomes negative with a value of -9.8 J/kg·K.

Figure 4 shows the temperature-dependence of magnetization divided by the applied magnetic field, parallel and perpendicular to the *c*-axis, namely, $M(T)/H$ with $H = 10$ kOe, for a single crystal of DyB₄. Similar to the HoB₄ case, there are two successive magnetic transitions at $T_{N2} = 13.0$ K and $T_{N1} = 20.5$ K for an applied magnetic field parallel and perpendicular to the *c*-axis, respectively³². It is determined that the origins of these two transitions are quite similar to those in HoB₄ and are responsible for the magnetic order and quadrupolar order. However, the types of their orderings in DyB₄ are distinct from the ones in HoB₄. At $T = T_{N1}$, collinear antiferromagnetic ordering is developed along the *c*-axis, while quadrupolar ordering is developed at $T = T_{N2}$, which accompanies the structural distortion and magnetic order in both the *ab*-plane and the *c*-axis²⁹.

The isothermal magnetization curves at various temperatures in the range of $2 \text{ K} \leq T \leq 50 \text{ K}$ with a field applied along the *c*-axis and perpendicular to the *c*-axis for DyB₄ are plotted in Fig. 5(a,b), respectively. The magnetizations along the *c*-axis at $T = 2$ K and 5 K undergo field-induced transitions near $H \approx 45$ kOe and the magnetic moment of a Dy³⁺ ion is observed to be $3.8 \mu_B$ at $H = 50$ kOe³³. Because the theoretical value of the Dy³⁺ ion moment is $10.6 \mu_B$, the transition is likely to be a meta-magnetic transition in the orbital ordered state, corresponding to the first meta-magnetic transition at $H = 25$ kOe in HoB₄. The isothermal curves are found to follow paramagnetic behaviour at $T = 20$ K and 50 K. On the other hand, the isothermal data, perpendicular to the *c*-axis, show typical antiferromagnetic features without meta-magnetic transitions.

The temperature dependences of the magnetic entropy change for DyB₄ is calculated using the isothermal magnetization data for a magnetic field applied along the *c*-axis and in the *ab* plane (Fig. 5) and are plotted in Fig. 6(a,b). For a field applied along the *c*-axis, a large positive entropy change, ΔS_M (50 kOe), is observed below $T = T_{N2}$ with a maximum value of 19.6 J/kg·K at $T = T_{N2}$, as shown in Fig. 6(a). The entropy change near $T = T_{N1}$ is relatively small and negative. On the other hand, there is no significant magnetic entropy change for a field applied in the *ab* plane with a positive ΔS_M (50 kOe) = 1.80 J/kg·K near $T = T_{N2}$ and a negative ΔS_M (50 kOe) = -3.40 J/kg·K near $T = T_{N1}$.

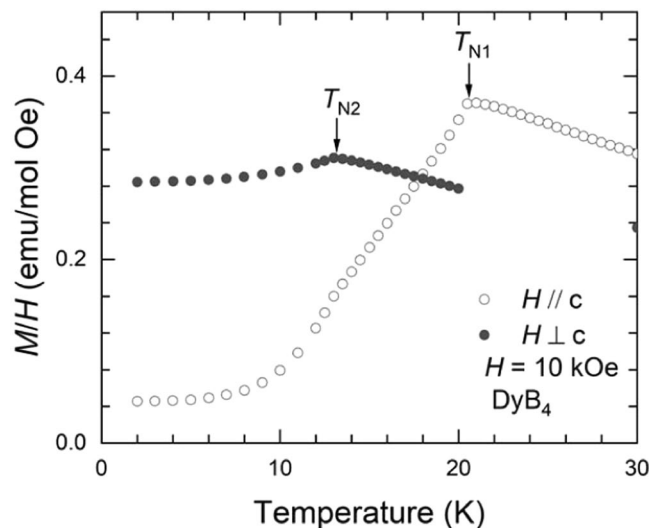


Figure 4. Temperature-dependent magnetization divided by an applied magnetic field, $H = 10$ kOe, parallel and perpendicular to the c -axis for DyB_4 .

It is quite interesting that the maximum entropy change (ΔS_M) occurs at $T = T_{N2}$ with the magnetic field of the meta-magnetic transition for both HoB_4 and DyB_4 . Because the meta-magnetic transition is a field-induced spin reorientation, which is strongly coupled with the quadrupole moment, a steep increase in ΔS_M near $T = T_{N2}$ with a maximum ΔS_M at $T = T_{N2}$ along the c -axis should be associated with the orbital ordering degeneracy release. In particular, the entropy change of HoB_4 at $T_{N2} = 5.7$ K increases as the field increases, reaching its maximum at the field change of 25 kOe and then decreasing with a further increase in the field change. Similarly, the entropy change of DyB_4 is maximized at $T_{N2} = 13.0$ K and the critical field $H = 45$ kOe, which is expected to be suppressed with a further increase of the field. This field dependence of the entropy change is quite unusual compared to the conventional behaviour, which originates purely from magnetic moments (unprecedented behaviour to our knowledge). Thus, the large magnetocaloric effect of both HoB_4 and DyB_4 near $T = T_{N2}$ is a consequence of the magnetic moment reorientation, strongly coupled with quadrupolar ordering in the presence of strong spin-orbit coupling.

To understand such behaviour of a large *inverse* MCE, it is important to note that the system is geometrically frustrated and metallic. Geometrical frustration and thus competing exchange interactions are crucial for inducing two successive magnetic transitions^{34,35}. In addition, the magnetic moment and quadrupole moment are strongly coupled and mediated via itinerant electrons in this metallic system. This leads to a sudden change in the magnetization near the critical field, especially at transition temperature T_{N2} , where the quadrupole moment is being developed. Within Landau theory, one can qualitatively understand this phenomena taking three order parameters into account, namely, the antiferromagnetic order (M_s), the ferroquadrupolar order (Q) and the uniform magnetization (M_u).

$$F(M_s, M_u, Q, H) = u_s M_s^4 + r_s M_s^2 + u_Q Q^4 + r_Q Q^2 \\ + u_u M_u^4 + r_u M_u^2 + g(H) M_u \\ F_{int}(M_s, M_u, Q) = w M_s^2 Q^2 + v M_u^2 Q^2 + l M_u^2 M_s^2$$

$F(M_s, M_u, Q, H)$ represents the Landau free energy with mass and quartic interaction terms for M_s , M_u and Q . In terms of the uniform magnetization, M_u has an additional term $g(H)M_u$ due to the dominant coupling with a magnetic field H . Here, the function $g(H)$ takes the magnetization jump at a critical field H_c into account, thus $g(H) = c \left(\text{Tanh} \left[\frac{H_c - H}{T} \right] - \text{Tanh} \left[\frac{H_c}{T} \right] \right)$, where c is some constant and T is the temperature. $F_{int}(M_s, M_u, Q)$ represents the Landau free energy for interactions between the order parameters at quartic levels.

The consecutive phase transitions can be explained by taking the mass terms $r_s = \frac{T - T_M}{T_M}$ and $r_Q = \frac{T - T_Q}{T_Q}$, where the system stabilizes the antiferromagnetic order and ferroquadrupolar order at T_M and T_Q , respectively ($T_Q < T_M$). Of course, these transition temperatures can be shifted in the presence of the interaction term $w M_s^2 Q^2$ in $F_{int}(M_s, M_u, Q)$. When the magnetic field is applied, the uniform magnetization M_u is being developed. In this case, the interaction terms in $F_{int}(M_s, M_u, Q)$ lead the magnitude of M_u to change non-monotonically near the transition temperatures T_M and T_Q . We set the parameters u_s , u_Q and u_u to be all positive for stability of the order parameters, and $r_u > 0$ when the ferromagnetism is absent without a field. For the interaction terms in $F_{int}(M_s, M_u, Q)$, we set $w < 0$, $v > 0$ and $l > 0$. Figure 6(c) shows the calculated entropy change as a function of temperature with different magnetic field strengths. When the field strength approaches the critical field H_c , the positive entropy change is maximized near the transition temperature of the quadrupolar order (T_Q). Such a positive entropy change exists only below the magnetic ordering temperature (T_M), with the negative entropy change

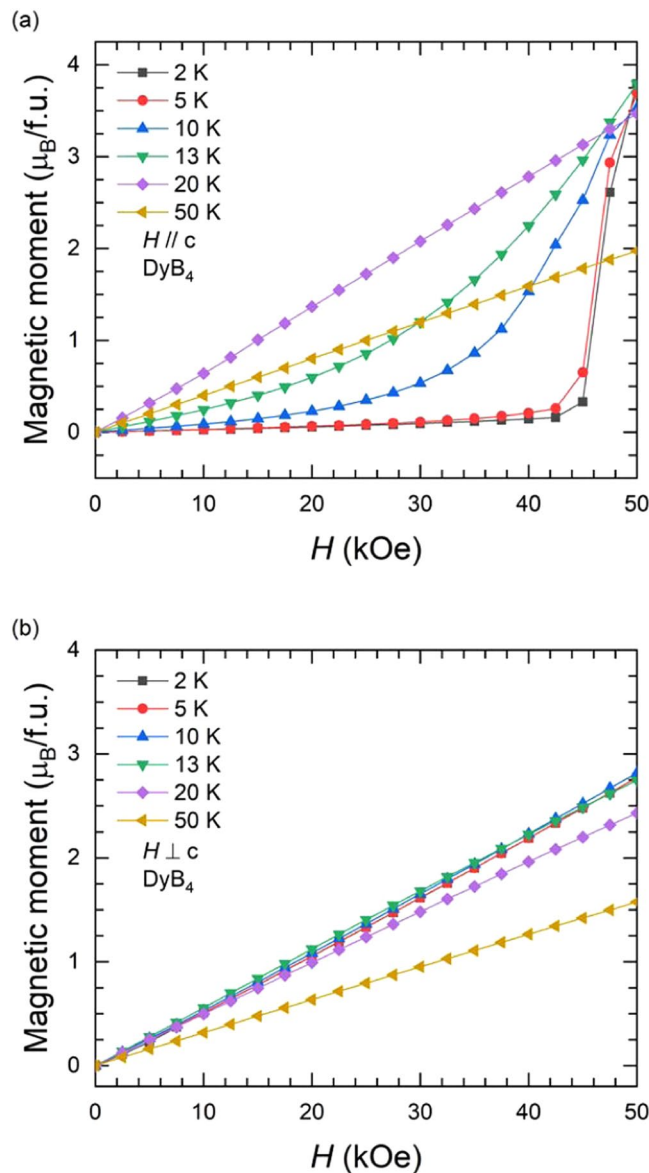


Figure 5. Magnetic field dependence of the isothermal magnetization at different temperatures in a range of $2\text{ K} \leq T \leq 100\text{ K}$ with applied field; (a) parallel and (b) perpendicular to the c -axis for DyB_4 .

shown for $T > T_M$, as expected for a conventional MCE. This behaviour is qualitatively in good agreement with the entropy change observed in rare-earth tetraborides DyB_4 and HoB_4 .

To observe the correlation of the field dependence of the entropy change with the spin-orbit interaction strength, a $\text{Dy}_{0.5}\text{Ho}_{0.5}\text{B}_4$ single crystalline specimen is synthesized. Figure 7(a) shows the temperature dependence of the magnetization with a magnetic field of $H = 10\text{ kOe}$ parallel and perpendicular to the c -axis. Two successive transitions at $T_{N1} = 13.8\text{ K}$ and $T_{N2} = 9.5\text{ K}$ are observed, which are in-between those of DyB_4 and HoB_4 , as expected. The entropy change for the field applied parallel to the c -axis is calculated from the isothermal magnetization data (see Supplementary Data) and is plotted in Fig. 7(b) as a function of temperature with various fields of $H = 10, 20, 30, 40,$ and 50 kOe . The maximum positive $\Delta S_M(40\text{ kOe}) (= 19.0\text{ J/kg}\cdot\text{K})$ is found near $T = T_{N2}$ with the field change of 40 kOe . This provides clear evidence that the critical field for the maximum entropy change is correlated with the quadrupole coupling strength and the magnetic ground state.

The data for three compounds (DyB_4 , $\text{Dy}_{0.5}\text{Ho}_{0.5}\text{B}_4$ and HoB_4) are summarized in Table 1. It is believed that the large positive entropy change near $T = T_{N2}$ is not due to a simple antiferromagnetic transition at $T = T_{N1}$, but instead due to the strong correlation between the quadrupole ordering and magnetic moment. There is no significant variation in the maximum ΔS_M values of the three compounds, indicating that the accumulated magnetic degeneracies due to a quadrupolar interaction with a magnetic dipole moment are similar for the three compounds. The critical field, i.e., the magnetic field at which the maximum entropy change is found, decreases gradually to be 50 kOe for DyB_4 , 40 kOe for $\text{Dy}_{0.5}\text{Ho}_{0.5}\text{B}_4$ and 25 kOe for HoB_4 . Because these fields are close to those for the field-induced meta-magnetic transitions, the critical field should be correlated with the coupling

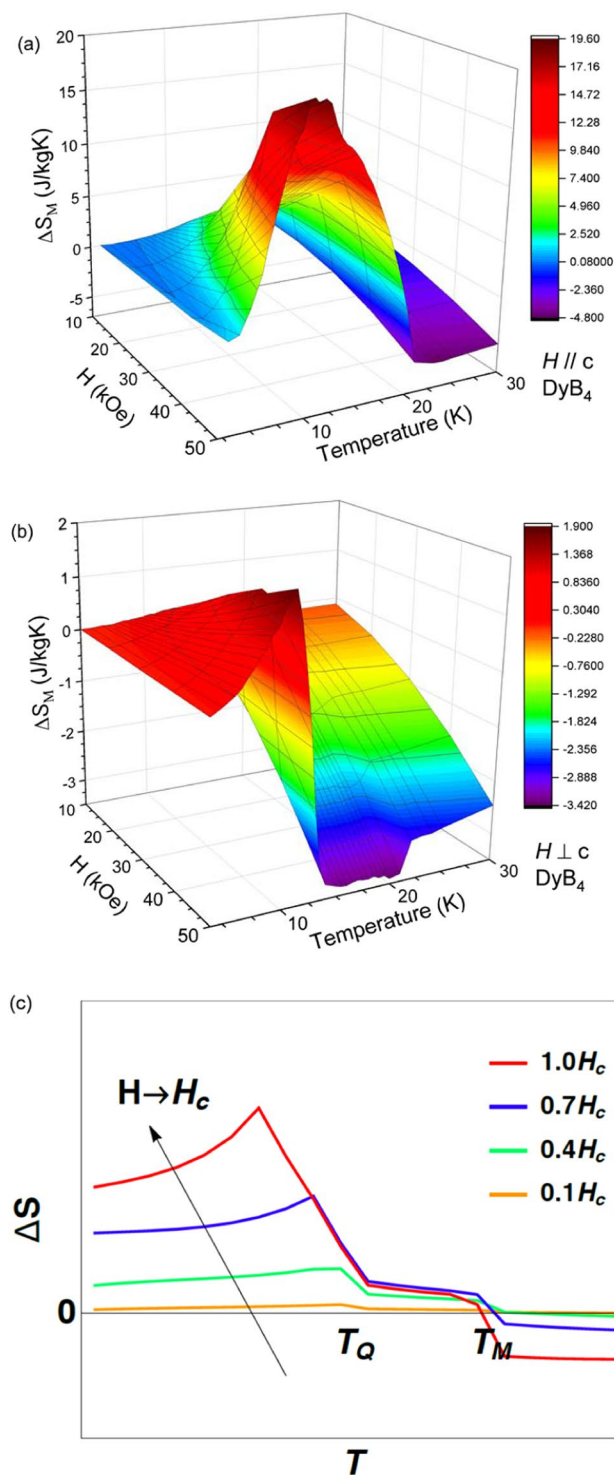


Figure 6. Temperature dependence of the magnetic entropy change of DyB_4 during various magnetic field changes of 10, 20, 30, 40 and 50 kOe; (a) parallel to the c -axis and (b) perpendicular to the c -axis. (c) Theoretical calculation of the entropy change based on the Landau free energy, which shows the agreement with the observed data in terms of the temperature and field (See the main text for more details).

strength between the magnetic and quadrupole moments. Thus, with a further increase in the magnetic field above the critical field, the effects of quadrupolar ordering on the magnetic entropy change, ΔS_M , would decrease, contrary to the conventional MCE.

For comparison, materials, which exhibit inverse MCE, are also listed in Table 1. A Hesler alloy, $\text{Ni}_{40.6}\text{Mn}_{43.4}\text{Sn}_{10.0}\text{Co}_{6.1}$ shows a positive entropy change of 29.5 J/kgK with the field change of 50 kOe during first order martensite transition and intermediate martensite transition with structural transformation³⁶. The perovskite

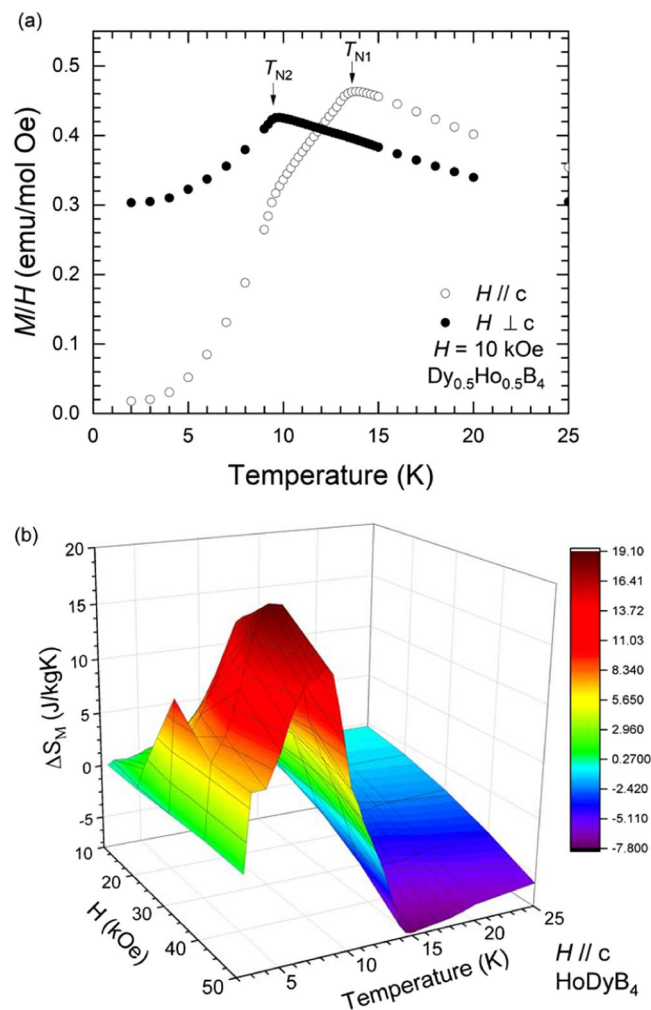


Figure 7. (a) Temperature-dependent magnetization divided by a magnetic field, $H = 10$ kOe, applied parallel and perpendicular to the c -axis for $\text{Dy}_{0.5}\text{Ho}_{0.5}\text{B}_4$. (b) Temperature-dependence of the magnetic entropy change in $\text{Dy}_{0.5}\text{Ho}_{0.5}\text{B}_4$ during various magnetic field changes of 10, 20, 30, 40 and 50 kOe, applied parallel to the c -axis.

	T_{N2} (K)	T_{N1} (K)	$T_{N1} - T_{N2}$ (K)	$+\Delta S_M$ (J/kgK)	H_{max} (kOe)
DyB_4	13	20.1	7.1	19.6	≈ 50
$\text{Dy}_{0.5}\text{Ho}_{0.5}\text{B}_4$	9.5	13.8	4.3	19.0	40
HoB_4	5.5	7.5	2	22.72	25
$\text{Ni}_{40.6}\text{Mn}_{43.3}\text{Sn}_{10.0}\text{Co}_{6.1}$	$T_M = 308$	$T_A = 323$	—	29.5	50
$\text{La}_{0.125}\text{Ca}_{0.875}\text{MnO}_3$	—	125	—	≈ 6.1	50
$\text{LaFe}_{12}\text{B}_6$	—	36	—	19	70

Table 1. Experimental data for single crystalline samples of $\text{Ho}_{1-x}\text{Dy}_x\text{B}_4$ and other materials with inverse MCE. T_{N2} : quadrupolar ordering temperature, T_{N1} : antiferromagnetic transition temperature, T_M : martensite transition temperature, T_A : austenite transition temperature ΔS_M : maximum entropy change, and H_{max} : field for maximum magnetic entropy change.

manganite, $\text{La}_{0.125}\text{Ca}_{0.875}\text{MnO}_3$, has complicate magnetic structure due to the interaction between antiferromagnetic super exchange and ferromagnetic double exchange couplings and shows a positive entropy change of ≈ 6.1 J/kgK with the field change of 50 kOe³⁷. A large inverse MCE is also observed in $\text{LaFe}_{12}\text{B}_6$ with the positive entropy change of 19 J/kgK with the field change of 70 kOe³⁸. The antiferromagnetic ground state is found to coexist with ferromagnetic state via field-induced first order magnetic transition. The amount of entropy changes of the materials is proportional to the applied field. Thus, the critical field dependence of entropy change in $\text{Ho}_{1-x}\text{Dy}_x\text{B}_4$ looks unique and interesting feature.

Conclusions

We have systematically investigated the magnetic entropy change, i.e., the MCE, and its correlation with multipolar phase transitions, for three compounds: DyB₄, Dy_{0.5}Ho_{0.5}B₄ and HoB₄. These three compounds exhibit common features of double phase transitions, where the magnetic order is developed at T_{N1} and the quadrupolar order is developed at T_{N2} ($T_{N1} \sim 20.5$ K, 13.8 K, 7 K and $T_{N2} \sim 13.0$ K, 9.5 K, 5.7 K for DyB₄, Dy_{0.5}Ho_{0.5}B₄ and HoB₄, respectively). Interestingly, an large positive entropy change, i.e., an *inverse* MCE, is observed near $T = T_{N2}$ as the magnetic field approaches the critical field of the meta-magnetic transitions (≈ 50 kOe, 40 kOe, and 25 kOe for DyB₄, Dy_{0.5}Ho_{0.5}B₄ and HoB₄, respectively). The maximum ΔS_M values are estimated as 19.6 J/kg·K, 19.0 J/kg·K and 22.7 J/kg·K for DyB₄, Dy_{0.5}Ho_{0.5}B₄ and HoB₄, respectively. While a conventional magnetic entropy change is observed at $T = T_{N1}$, as is expected for the conventional MCE, a large *inverse* MCE observed at $T = T_{N2}$ is quite peculiar. Furthermore, these maximum values of ΔS_M for Dy_{1-x}Ho_xB₄ are very close to the largest values reported among the magnetocaloric materials in the low-field region ($H \leq 20$ kOe) and the largest reported for antiferromagnetic compounds.

Such an exotic inverse MCE is unique, originating from an interplay of a strong spin-orbit coupling and geometric frustration. Strong spin-orbit coupling and crystal field splitting lead to the formation of a pseudo-quartet for low lying states and allows for multipolar degrees of freedom, including both magnetic dipoles (linear in total angular momentum J) and quadrupoles (quadratic in J). In rare-earth tetraborides, such multipolar degrees of freedom lie in a geometrically frustrated Shastry-Sutherland lattice and interact with one another via itinerant electrons. This induces consecutive double phase transitions in the presence of strong coupling between magnetic dipoles and quadrupoles. Thus, the magnetization change as a function of temperature is expected to be enhanced at $T = T_{N2}$ with the critical magnetic field of the meta-magnetic transition, resulting in a large positive entropy change and abnormal field dependence. This new mechanism opens a potential pathway to understanding the physical origin of a large *inverse* MCE in rare earth tetraborides. In addition, it enables us to enhance the controllability of the MCE with several parameters and applications for other candidate materials with strong spin-orbit coupling.

Method

The single crystals of RB₄ ($R = \text{Dy}$ and Ho) are prepared by a high-temperature metal flux method using the Al flux^{29,30}. A stoichiometric mixture of rare earth metals ($\geq 99.9\%$, China Rare Metal Material Co., LTD.) and boron pieces (99.9%, RND Korea) are placed in an alumina crucible (99.8%, Samhwa Ceramic Company) together with the Al (99.999%, RND Korea) flux at a mass ratio of RB₄: Al = 1: 50. The mixture is placed in a heated tube furnace with an MoSi₂ heating element. The furnace is heated at a rate of 300 °C per hour to 1650 °C under a high-purity argon atmosphere after dehydration and cooled slowly at a rate of 4.8 °C per hour to 650 °C. The single crystals are separated from the flux by dissolving the excess Al in NaOH.

The crystal structures are characterized using x -ray diffraction measurements (XRD; Rigaku D/MAX-2500 with a Cu target) at room temperature. The XRD data are collected on pulverized single crystals of DyB₄ and HoB₄. The XRD patterns show a single phase of DyB₄ and HoB₄ without any observable impurity peaks. The Bragg peak positions are in good agreement with the tetragonal symmetry of the ThB₄-type structure and space group $P4/mbm$ (#127)^{30,32}. The lattice parameters are determined from LeBail refinements using FULLPROF software. The refined lattice parameters are $a = 7.099(5)$ Å and $c = 4.015(9)$ Å for DyB₄ and $a = 7.083(8)$ Å and $c = 4.005(1)$ Å for HoB₄. The temperature- and field-dependent magnetizations are measured using a superconducting quantum interference device magnetometer (SQUID; Quantum Design MPMS XL).

Received: 3 April 2019; Accepted: 2 January 2020;

Published online: 21 January 2020

References

- Gschneidner, K. A. Jr. & Pecharsky, V. K. Thirty years of near room temperature magnetic cooling: Where we are today and future prospects. *Int. J. Ref.* **31**, 945–961 (2008).
- Pakhira, S., Mazumdar, C., Ranganathan, R. & Avdeev, M. Magnetic frustration induced large magnetocaloric effect in the absence of long range magnetic order. *Sci. Rep.* **7**, 7367 (2017).
- Midya, A., Khan, N., Bhoi, D. & Mandai, P. Giant magnetocaloric effect in magnetically frustrated EuHo₂O₄ and EuDy₂O₄ compounds. *Appl. Phys. Lett.* **101**, 132415 (2012).
- Balli, M., Roberge, B., Fournier, P. & Jandl, S. Review of the magnetocaloric effect in RMnO₃ and RMn₂O₅ Multiferroic Crystals. *Crystals* **7**, 44 (2017).
- de Oliveria, I. G., Caldas, A., Nobrega, E. P., de Oliveria, N. A. & von Ranke, P. J. The influence of the quadrupolar interaction in the magnetocaloric effect. *Solid State Commun.* **114**, 487–491 (2000).
- von Ranke, P. J. *et al.* The influence of quadrupolar interaction on the magnetocaloric effect in PrMg₂. *J. Alloys. Compd.* **440**, 46–50 (2007).
- von Ranke, P. J. *et al.* Anomalous magnetocaloric effect in YbAs associated with the giant quadrupolar interaction. *Phys. Rev. B* **63**, 02442 (2000).
- Kusunose, H. Description of Multipole in f -Electron Systems. *J. Phys. Soc. Jpn.* **77**, 064710 (2008).
- Kuramoto, Y., Kusunose, H. & Kiss, A. Multipole Orders and Fluctuations in Strongly Correlated Electron Systems. *J. Phys. Soc. Jpn.* **78**, 072001 (2009).
- Preleiderer, C. Superconducting phases of f -electron compounds. *Rev. Mod. Phys.* **81**, 1551 (2009).
- Santini, P., Carretta, S. & Amoretti, G. Multipolar interactions in f -electron systems: The paradigm of actinide dioxides. *Rev. Mod. Phys.* **81**, 807 (2009).
- Morin, P., Schmitt, D. & du Tremolet de Lacheisserie, E. Magnetic and quadrupolar properties of PrPb₃. *J. Magn. Magn. Mater.* **30**, 257–264 (1982).
- Caciuffo, R. *et al.* Multipolar ordering in NpO₂ below 25 K. *J. Phys: Condens. Matter* **15**, S2287 (2003).
- Chandra, P., Coleman, P., Mydosh, J. A. & Tripathi, V. Hidden orbital order in the heavy fermion metal URu₂Si₂. *Nature* **417**, 831–834 (2002).
- Schmidt, A. R. *et al.* Imaging the Fano lattice to 'hidden order' transition in URu₂Si₂. *Nature* **465**, 570–576 (2010).

16. Lee, S., Paramakanti, A. & Kim, Y. B. Optical gyrotropy in quadrupolar Kondo systems. *Phys. Rev. B* **91**, 041104 (2015).
17. Kitagawa, J., Takeda, N. & Ishikawa, M. Possible quadrupolar ordering in a Kondo-lattice compound $\text{Ce}_3\text{Pd}_{20}\text{Ge}_6$. *Phys. Rev. B* **53**, 5101 (1996).
18. Okuyama, D., Matsumura, T., Nakao, H. & Murakami, Y. Quadrupolar frustration in Shastry-Sutherland lattice of DyB_4 studied by resonant x-ray scattering. *J. Phys. Soc. Jpn.* **74**, 2434–2437 (2005).
19. Matsumura, T., Okuyama, D., Mouri, T. & Murakami, Y. Successive magnetic phase transition of component orderings in DyB_4 . *J. Phys. Soc. Jpn.* **80**, 074701 (2011).
20. Shastry, B. S. & Sutherland, B. Exact ground state of a quantum mechanical antiferromagnet. *Physical B*. **108B**, 1069–1070 (1981).
21. Buschow, K. H. J. & Creighton, J. H. N. Magnetic properties of rare earth tetraborides. *J. Chem. Phys.* **57**, 3910 (1972).
22. Schäfer, W., Will, G. & Buschow, K. H. J. The magnetic structure of the rare earth tetraborides ErB_4 and DyB_4 . *J. Chem. Phys.* **64**, 5 (1976).
23. Etourneau, J. *et al.* The magnetic and electrical properties of some rare earth tetraborides. *J. Less-Common Metals* **67**, 531–539 (1979).
24. Gianduzzo, J. C. *et al.* Anisotropy and magnetic phase transitions in the rare earth tetraborides TbB_4 , HoB_4 and ErB_4 . *J. Less-Common Metals* **82**, 29–35 (1981).
25. Fisk, Z., Maple, M. B., Johnston, D. C. & Woolf, L. D. Multiple phase transitions in rare earth tetraborides at low temperature. *Solid State Comm.* **39**, 1189–1192 (1981).
26. Okuyama, D., Matsumura, T., Nakao, H. & Murakami, Y. Quadrupolar ordering and structural phase transition in DyB_4 with geometrical frustration. *J. Phys. Soc. Jpn.* **75**, 198–200 (2005).
27. Ji, S. *et al.* Resonant X-ray scattering study of quadrupole-strain coupling in DyB_4 . *Phys. Rev. Lett.* **99**, 076401 (2007).
28. Okuyama, D. *et al.* Competition of magnetic and quadrupolar order parameters in HoB_4 . *J. Phys. Soc. Jpn.* **77**, 044709 (2008).
29. Sim, H. *et al.* Spontaneous structural distortion of the metallic Shastry-Sutherland system DyB_4 by quadrupole-spin-lattice coupling. *Phys. Rev. B* **94**, 195128 (2016).
30. Kim, J. Y., Cho, B. K. & Han, S. H. Anisotropic magnetic phase diagrams of HoB_4 single crystal. *J. Appl. Phys.* **105**, 07E116 (2009).
31. Brunt, D. *et al.* Field-induced magnetic states in holmium tetraboride. *Phys. Rev. B* **95**, 024410 (2017).
32. Kang, B. Y., Kim, J. Y., Choi, H. Y. & Cho, B. K. Anomalous weak ferromagnetism in the magnetically frustrated system $\text{R}_{1-x}\text{Y}_x\text{B}_4$ ($\text{R} = \text{Tb}$ and Dy). *Phys. Rev. B* **91**, 024414 (2015).
33. Watanuki, R., Mitamura, H., Sakaikbara, T., Sato, G. & Suzuki, K. Physical properties and phase diagram of geometrically quadrupolar frustrated system DyB_4 . *Physica B* **378–380**, 594 (2006).
34. Lee, S., Trebst, S., Kim, Y. B. & Paramakanti, A. Landau theory of multipolar order in $\text{Pr}(\text{Y})_2\text{X}_{20}$ Kondo materials ($\text{Y} = \text{Ti, V, Rh, Ir}$; $\text{X} = \text{Al, Zn}$). *Phys. Rev. B* **98**, 134447 (2018).
35. Freyer, F. *et al.* Two-stage multipolar ordering in $\text{PrT}_2\text{Al}_{20}$ Kondo materials. *Phys. Rev. B* **97**, 115111 (2018).
36. Zhang, X., Zhang, H., Qian, M. & Geng, L. Enhanced magnetocaloric effect in Ni-Mn-Sn-Co alloys with two successive magnetostructural transformations. *Sci. Rep.* **8**, 8235 (2018).
37. Biswas, A., Samanta, T., Banerjee, S. & Das, I. Inverse magnetocaloric effect in polycrystalline $\text{La}_{0.125}\text{Ca}_{0.875}\text{MnO}_3$. *J. Phys.: Condens. Matter* **21**, 506005 (2009).
38. Diop, L. V. B. & Isnard, O. Inverse and normal magnetocaloric effects in $\text{LaFe}_{12}\text{B}_6$. *J. Appl. Phys.* **119**, 213904 (2016).

Acknowledgements

M.S. Song is grateful to D.Y. Kim and J.W. Lee at Gwangju Institute of Science and Technology, Republic of Korea, for experimental assistance. This work was supported by LG Electronics Inc. and the National Research Foundation of Korea (NRF), funded by the Ministry of Science, ICT & Future Planning (No. NRF-2015M3A9B8032703 and No. NRF-2017R1A2B2008538). S.B.L. is supported by the KAIST start-up and the National Research Foundation Grant (NRF-2017R1A2B4008097).

Author contributions

M.S. Song, K.K. Cho and B.Y. Kang designed and carried out the experiments, analysed the data. S.B. Lee developed theoretical model for the interpretation the data. M.S. Song and S.B. Lee prepared the manuscript under the supervision of B.K. Cho.

Competing interests

The authors declare no competing interests.

Additional information

Supplementary information is available for this paper at <https://doi.org/10.1038/s41598-020-57621-7>.

Correspondence and requests for materials should be addressed to B.K.C.

Reprints and permissions information is available at www.nature.com/reprints.

Publisher's note Springer Nature remains neutral with regard to jurisdictional claims in published maps and institutional affiliations.



Open Access This article is licensed under a Creative Commons Attribution 4.0 International License, which permits use, sharing, adaptation, distribution and reproduction in any medium or format, as long as you give appropriate credit to the original author(s) and the source, provide a link to the Creative Commons license, and indicate if changes were made. The images or other third party material in this article are included in the article's Creative Commons license, unless indicated otherwise in a credit line to the material. If material is not included in the article's Creative Commons license and your intended use is not permitted by statutory regulation or exceeds the permitted use, you will need to obtain permission directly from the copyright holder. To view a copy of this license, visit <http://creativecommons.org/licenses/by/4.0/>.

© The Author(s) 2020